

Corrections to the gravitational wave phasing

Shaoqi Hou,^{*} Xi-Long Fan,[†] and Zong-Hong Zhu[‡]

School of Physics and Technology, Wuhan University, Wuhan, Hubei 430072, China

(Dated: November 12, 2019)

The gravitational wave, traveling a long cosmological distance to reach the interferometers, interacts with the cosmological background, so generally speaking, its amplitude and phase are modified in some nontrivial way. As the sensitivity of the interferometers are improved, one may detect the corrections to the short-wavelength approximation, which naturally includes the information of the cosmological evolution. In this work, the calculation of the Newman-Penrose variable Ψ_4 has been done to show that there are two new corrections to the short-wavelength approximation. One formally occurs at the 1st post-Newtonian order, but is highly suppressed by the Hubble parameters; the other occurs at the 5th post-Newtonian order, which is due to the variation of the amplitude. The first correction contains the evolution of the universe, but it may not be easily detected. The second one indicates that the short-wavelength approximation has to be corrected, when the more accurate waveforms with the higher order post-Newtonian terms are calculated.

I. INTRODUCTION

The detection of gravitational waves (GWs) by LIGO/Virgo collaborations [1–7] confirmed the prediction of general relativity (GR) [8], which also marked the new era of the GW astronomy and the multi-messenger astronomy. The GW is a probe to the nature of the gravity in the dynamical, high speed regime. For example, the detection of the polarizations of the GW would exclude either GR or some alternative metric theories of gravity [9–12]. KAGRA [13, 14] has now joint LIGO/Virgo network, and their observations might put stronger constraint on the GW polarization content. Moreover, the measurement of the GW speed from GW170817 and GRB 170817A [5, 15–17] has already severally constrained some of the alternatives [11, 18–25]. With the advent of the space-borne and more advanced 3rd generation detectors such as Einstein Telescope [26], more GW events can be detected, and our understanding of the nature of gravity, and thereby other phenomena such as the cosmology, can be greatly improved.

GWs produced by a compact binary system travel long distances to reach interferometers. Several interesting propagation effects occur, which have some influences on the amplitude and the phase of the GW. For the GWs detected by the interferometers, their wavelengths λ_{gw} are much smaller than the Hubble radius $1/H$, so the short-wavelength limit can be safely applied [27]. When there are no obstacles on the way, the GW amplitude decays, inversely proportional to the luminosity distance [28]. This is due to the conservation of the number of the gravitons and the expansion of the universe [29]. When there are gravitational lenses near the trajectories of the GWs, the gravitational lensing takes place [30–34]. This causes the magnification of the gravitational amplitudes

[35], the rotation of the polarization plane [32, 36], and the formation of the beat pattern of the strain [37].

One of the most famous applications of the GW to cosmology is to measure the luminosity distance very accurately, that is, the GW sources are the standard sirens [38, 39]. The first standard siren measurement gave $H_0 = 70.0^{+12.0}_{-8.0} \text{ km s}^{-1}\text{Mpc}^{-1}$ based on GW170817 [40], which is consistent with previous measurements, and was improved modestly in a recent joint estimate using the detections made in the first and the second observing runs of LIGO/Virgo [41]. Within 5 years, the Hubble constant can be constrained to 2 percent level with LIGO/Virgo, probably clarifying the Hubble tension and shedding light on the dark matter [42]. In order to use the luminosity distance to study some cosmological parameters, one needs to know the redshift of the GW source, which cannot be read off from the waveform obtained based on the short-wavelength approximation. This is because in the leading order in the short-wavelength approximation, the gravitational waveform can be put in a form which seems independent of the source redshift z . Recently, several works took the evolution of the universe into account, and the waveform carries the information of the evolution. For example, Refs. [43, 44] considered the time dependence of z , which leads to a nontrivial time evolution of the measured GW frequency. The resultant waveform acquires a modification, related to the Hubble parameter and z . This allows to merely use the GW observation to study cosmology, in principle. However, although this effect occurs at the -4PN order, it is very small, compared to the correction due to the peculiar acceleration of the binary system as discussed in Ref. [45]. So it is not very efficient to make use of this effect to measure z .

Besides the effect of the cosmological evolution on z , one may consider the other corrections to the short-wavelength approximation, which might occur at the same order (in $\lambda_{\text{gw}}H$) as the time varying redshift, and were ignored in Refs. [43–45]. In the short-wavelength approximation, one writes the metric perturbation in a form with a slowly varying amplitude and a rapidly oscillating

^{*} hou.shaoqi@whu.edu.cn

[†] xilong.fan@whu.edu.cn

[‡] zhuzh@whu.edu.cn

phase. Therefore, the GW strain measured by the interferometer is simply proportional to the amplitude at the leading order in $\lambda_{\text{gw}}H$. However, the amplitude varies over space and time, owing to (1) the orbital evolution of the binary system, and (2) the cosmological expansion. Taking the changing amplitude into account, one finds out that the measured GW amplitude is modified, as naturally expected. In addition, one also effectively obtains some new corrections to the phase. Since the interferometers are very sensitive to the GW phasing, one may want to ignore the amplitude correction but focus on the corrections to the phase.

By directly calculating the Newman-Penrose variable Ψ_4 , taking the variation of the amplitude into account, one discovers that the variation of the amplitude induces a dephasing in the time domain. The dephasing consists of two parts. The first is due to the orbital decay of the binary system, so it becomes stronger as time flies. The second comes from the cosmological evolution, and depends on the Hubble parameters. As the GW frequency increases, the second contribution becomes smaller and smaller, as $\lambda_{\text{gw}}H$ is smaller and smaller. In terms of the counting of the post-Newtonian (PN) order, the first effect is at the 5PN order, while the second is formally at the 1PN order. In the above calculation, we ignored the peculiar motion of the binary system and the inhomogeneities of the universe, which were properly considered in Ref. [45]. Since the 1PN correction discussed in this work also carries a factor of Hubble parameters, it is much smaller than the -4 PN order correction discovered in Refs. [43–45], so it can also be ignored. The 5PN order correction is greater than the 1PN order one, especially in the the frequency bands of ground-based interferometers. This correction may be taken into account for more accurate modeling of the GW phase for future advanced detectors.

The tidal deformation of neutron stars breaks the degeneracy between the source masses and z , also making the electromagnetic counterpart dispensable [46, 47]. This effect induces corrections to the phase at the 5PN and 6PN orders, but these corrections have large coefficients such that their numerical values are comparable to the 3PN and 3.5PN order terms. The method analyzed in Refs. [46, 47] relies on the knowledge of the neutron star equations of state (EoS), and the predicted accuracy of the redshift measurement is at a few tens percentage level. The tidal deformability of neutron stars can also be used to obtain the EoS, which requires the accurate waveform at the high PN orders [48]. The 5PN order correction discovered in this work would inevitably affect the determination of the source redshift and the EoS of neutron stars.

This work is organized in the following way. In Sec. II, the propagation of the GW in the Friedmann-Robertson-Walker (FRW) spacetime is derived to obtain the evolution equations for the GW amplitudes in Sec. II A. Then, the subleading order GW amplitude is explicitly calculated in Sec. II B for the GW generated by a quasi-

circular, nonspinning binary star system. The Weyl tensor is thus computed in order to reveal the corrections due to the varying amplitudes in Sec. II C. In Sec. III, the time-domain waveform obtained in the previous section is Fourier transformed. The time dependence of the GW frequency is determined in Sec. III A, by mainly reviewing the derivations in Ref. [45]. After that, the stationary-phase approximation is applied to result in the waveform in the frequency domain. Finally, Sec. IV summarizes this work. In this work, the geometrized units are used with $G = c = 1$.

II. GRAVITATIONAL WAVES IN THE COSMOLOGICAL BACKGROUND

In this section, the propagation of the GW in the spatially flat FRW background will be analyzed. The GW comes from a binary system, and travels in the universe, so it interacts with the cosmological background. The detected GW differs from the initial one in its amplitude and phase. The evolution of the GW can be studied in the short-wavelength approximation, as the GW wavelengths detectable by interferometers are much smaller than the Hubble scale. In the leading order of this approximation, the effects of the cosmological background include only the decay of the amplitude with the luminosity distance, and the redshift of the frequency. However, the cosmological evolution, especially the redshift, is completely hidden in the expression for the waveform, once it is written in terms of some locally measurable quantities. If one goes beyond the leading order short-wavelength approximation, the cosmological evolution would affect the waveform in an explicit way. So in principle, it is not necessary to find an electromagnetic counterpart in order to study cosmology.

A. The evolution equations

In this subsection, the evolution equations of the GW will be derived up to the first order in the short-wavelength approximation. The background metric, the FRW metric, is given by [49]

$$ds^2 = a^2(\eta)[-d\eta^2 + \delta_{jk}dx^j dx^k], \quad (1)$$

where $a(\eta)$ is the scale factor and $\eta = \int dt/a(t)$ is the conformal time. The GW is the tensor perturbation h_{jk} to the above metric, and the perturbed metric is

$$ds'^2 = a^2(\eta)[-d\eta^2 + (\delta_{jk} + h_{jk})dx^j dx^k]. \quad (2)$$

It satisfies the following equation of motion [50],

$$h''_{jk} + 2\mathcal{H}h'_{jk} - \nabla^2 h_{jk} = 0, \quad (3)$$

where the prime means the derivative with respect to η , and $\mathcal{H} = a'/a$. $\nabla^2 = \partial_j \partial^j$ is the Laplacian for the 3-Euclidean metric. The tensor h_{jk} is transverse-traceless,

namely,

$$\partial^k h_{jk} = 0, \quad h = \delta^{jk} h_{jk} = 0. \quad (4)$$

Usually, in the cosmology literature, one Fourier transformations h_{jk} as the FRW metric possesses the translation symmetry. However, for our purpose, we would like to expand h_{jk} in the following way,

$$h_{jk} = \Re \left[(A_{jk} + \epsilon B_{jk} + \dots) e^{-i\Phi/\epsilon} \right], \quad (5)$$

where $\epsilon \sim \lambda_{\text{gw}} H \ll 1$ for the GW detectable by the interferometers, and \Re means to take the real part. Substituting this expansion into Eq. (3), one finds out that at the leading order $[O(1/\epsilon^2)]$,

$$-(l_0)^2 + \vec{l}^2 = 0, \quad (6)$$

where $l_\mu = \partial_\mu \Phi$ is the wave vector, and \vec{l} represents its spatial part. So the GW still propagates at the speed of light in the cosmological background. At the next order $[O(1/\epsilon)]$, one obtains the evolution equation for A_{jk} ,

$$\tilde{l}^\mu \partial_\mu A_{jk} + \frac{1}{2} A_{jk} \partial_\mu \tilde{l}^\mu - a \mathcal{H} u^\mu l_\mu A_{jk} = 0, \quad (7)$$

where $u^\mu = \delta_0^\mu / a$ is the 4-velocity of the comoving fluid in the conformal coordinates. Finally, the evolution of B_{jk} is given by,

$$\begin{aligned} & \tilde{l}^\mu \partial_\mu B_{jk} + \frac{1}{2} B_{jk} \partial_\mu \tilde{l}^\mu - a \mathcal{H} u^\mu l_\mu B_{jk} \\ & = -i \left(\frac{1}{2} \partial_\mu \partial^\mu A_{jk} - a \mathcal{H} u^\mu \partial_\mu A_{jk} \right), \end{aligned} \quad (8)$$

at the order $O(\epsilon^0)$. The transverse-traceless conditions (4) become

$$\tilde{l}^k A_{jk} = 0, \quad \tilde{l}^k B_{jk} + i \partial^k A_{jk} = 0, \quad (9)$$

$$\delta^{jk} A_{jk} = \delta^{jk} B_{jk} = 0. \quad (10)$$

These relations resemble those in Ref. [51]. Note that $\tilde{l}^\mu = \eta^{\mu\nu} l_\nu$, not raised by the background spacetime metric. So we put a tilde above the kernel symbol l . In the following, any quantities that can be raised or lowered by $\eta^{\mu\nu}$ and $\eta_{\mu\nu}$ carry the tilde symbol. It should also be notified that all the evolution equations and the gauge conditions are expressed in terms of the partial derivatives. So this suggests that it would be easier to do the calculation in the unphysical spacetime which is flat.

Furthermore, to calculate the evolutions of A_{jk} and B_{jk} , it is more convenient to use the spherical coordinate system. Suppose that the GW emits from the origin of the coordinate system, then a suitable tetrad basis

$\{\tilde{e}_\alpha^\mu\} = \{\tilde{l}^\mu, \tilde{n}^\mu, \tilde{x}^\mu, \tilde{y}^\mu\}$ can be chosen to be

$$\tilde{l}^\mu = \gamma_0 (1, 1, 0, 0), \quad (11)$$

$$\tilde{n}^\mu = \frac{1}{2\gamma_0} (1, -1, 0, 0), \quad (12)$$

$$\tilde{x}^\mu = \left(0, 0, \frac{1}{r}, 0 \right), \quad (13)$$

$$\tilde{y}^\mu = \left(0, 0, 0, \frac{1}{r \sin \theta} \right), \quad (14)$$

where r is the comoving distance to the origin where the source is, and γ_0 is a constant, which can be fixed later. Measured by $\eta_{\mu\nu}$, these vectors satisfy $-\tilde{l}^\mu \tilde{n}_\mu = \tilde{x}^\mu \tilde{x}_\mu = \tilde{y}^\mu \tilde{y}_\mu = 1$ and the remaining contractions vanish. In addition, $\tilde{l}^\nu \partial_\nu \tilde{e}_\alpha^\mu = 0$. Calculations shows that $\partial_\mu \tilde{l}^\mu = 2\gamma_0/r$. Write $A_{jk} = A^+ \tilde{e}_{jk}^+ + A^\times \tilde{e}_{jk}^\times$ with $P = +, \times$, and

$$\tilde{e}_{jk}^+ = \tilde{\mathbf{x}}_j \tilde{\mathbf{x}}_k - \tilde{\mathbf{y}}_j \tilde{\mathbf{y}}_k, \quad (15)$$

$$\tilde{e}_{jk}^\times = \tilde{\mathbf{x}}_j \tilde{\mathbf{y}}_k + \tilde{\mathbf{y}}_j \tilde{\mathbf{x}}_k, \quad (16)$$

where the bold symbols represent the spatial parts. Here, neither of A^P has the tilde symbol overhead, since they represent the physical amplitudes. One knows that $\tilde{l}^\mu \partial_\mu \tilde{e}_{jk}^P = 0$. Then, Eq. (7) comes

$$\frac{\gamma_0}{ar} \frac{d}{dr} (ar A^P) = 0. \quad (17)$$

Here, $r(= \eta)$ is used to parameterize the null geodesic. This gives the usual law of the decay of the amplitude $A^P \propto 1/ar$.

Now, in order to calculate B_{jk} , one wants to expand it in the following way

$$B_{jk} = \sum_{P=+, \times} B^P \tilde{e}_{jk}^P + B^x \tilde{e}_{jk}^x + B^y \tilde{e}_{jk}^y, \quad (18)$$

where

$$\tilde{e}_{jk}^x = \tilde{\mathbf{x}}_j \tilde{\mathbf{l}}_k + \tilde{\mathbf{l}}_j \tilde{\mathbf{x}}_k, \quad (19)$$

$$\tilde{e}_{jk}^y = \tilde{\mathbf{y}}_j \tilde{\mathbf{l}}_k + \tilde{\mathbf{l}}_j \tilde{\mathbf{y}}_k. \quad (20)$$

Here, that B_{jk} can be expanded in such a more general form than A_{jk} is due to the gauge conditions (9) and (10) it satisfies. The explicit form of B_{jk} will be determined in the next subsection.

B. The gravitational wave generated by a binary system

In the vicinity of a binary system, it is possible to find a local Lorentz frame where the cosmological evolution barely affects the orbital motion of the stars to a good approximation. Suppose the orbit lies in the xOy plane of this frame, and let the stars have masses m_1 and m_2 . The spins are supposed to be zero. They move around

each other in a circular orbit at the angular frequency ω_e . Then the GW emitted is given by $\bar{h}_{0\mu} = 0$ and

$$\bar{h}_{jk} = \Re \left[\mathcal{A}_e e^{-i\Phi} \begin{pmatrix} -1 & -i & 0 \\ -i & 1 & 0 \\ 0 & 0 & 0 \end{pmatrix} \right], \quad (21)$$

$$\mathcal{A}_e = \frac{4\mathcal{M}_e}{a_e r_e} (\mathcal{M}_e \omega_e)^{2/3}, \quad (22)$$

where $\mathcal{M}_e = (m_1 m_2)^{3/5} / (m_1 + m_2)^{1/5}$ is the chirp mass, and $\Phi = -2 \int_t^{t_c} \omega_e(t') dt' + \Phi_c$ is the orbital phase with Φ_c the fiducial coalescence phase at the fiducial coalescence time t_c . The constant γ_0 can be fixed to be $\gamma_0 = 2\omega_e a_e$ such that l^0 [52] is the angular frequency of the GW. Here, we only take the leading order amplitude in the Newtonian approximation for simplicity. The extension of the current calculation to higher order post-Newtonian (PN) terms is straightforward but tedious. At some arbitrary distance r , the leading order wave amplitude is

$$\begin{aligned} \mathcal{A}(\eta - r, \theta, \phi) &= \frac{4\mathcal{M}_e}{ar} (\mathcal{M}_e \omega_e)^{2/3} \\ &= \frac{4\mathcal{M}}{d_L} (\pi \mathcal{M} f)^{2/3}, \end{aligned} \quad (23)$$

where d_L is the luminosity distance, $\mathcal{M} = (1+z)\mathcal{M}_e$ is the redshifted chirp mass and $f = \omega_e / \pi(1+z)$ is the measured GW frequency. On the right hand side, \mathcal{A} is explicitly written as a function of $u = \eta - r$, $\theta = \iota$ (the inclination angle) and ϕ . Along the GW ray, u is a constant, so the decay of the GW is due to the increase of the luminosity distance $d_L = ar(1+z)$. At a fixed radial location $r = \text{const.}$, the orbital frequency ω_e increases, which overcomes the growth in a , so the GW amplitude actually increases.

Now, one is ready to calculate B_{jk} . One should first use the second expression in Eq. (9) to easily obtain

$$B^x = -i \frac{4\mathcal{M}_e}{\gamma_0^2 ar^2} (\mathcal{M}_e \omega_e)^{2/3} e^{i2\phi} \sin 2\theta, \quad (24)$$

$$B^y = \frac{8\mathcal{M}_e}{\gamma_0^2 ar^2} (\mathcal{M}_e \omega_e)^{2/3} e^{i2\phi} \sin \theta, \quad (25)$$

which both decay as $1/r^2$. So neither of them represents the radiation, and they will be ignored in the following calculation.

Then, one can use Eq. (8) to calculate B^P ($P = +, \times$). After some tedious manipulations, one finds out that

$$B^+ = i \frac{\mathcal{M}_e}{\gamma_0 ar} (\mathcal{M}_e \omega_e)^{2/3} e^{i2\phi} E(\eta) (1 + \cos^2 \theta), \quad (26)$$

$$B^\times = -\frac{2\mathcal{M}_e}{\gamma_0 ar} (\mathcal{M}_e \omega_e)^{2/3} e^{i2\phi} E(\eta) \cos \theta. \quad (27)$$

Here, the function $E(\eta)$ is

$$E(\eta) = \mathcal{H} - \mathcal{H}_e + \int_{\eta_e}^{\eta} \mathcal{H}^2(\eta') d\eta' + \frac{4}{r} - \frac{4}{r_e}, \quad (28)$$

in which, $\frac{4}{r} - \frac{4}{r_e}$ can be dropped. In terms of $H = \dot{a}/a$ with dot denoting the derivative with respect to t , B^P can also be written as

$$B^+ = i \frac{\mathcal{M}^2 (\pi \mathcal{M} f)^{-1/3}}{d_L} e^{i2\phi} E'(t) \frac{1 + \cos^2 \theta}{2}, \quad (29)$$

$$B^\times = -\frac{\mathcal{M}^2 (\pi \mathcal{M} f)^{-1/3}}{d_L} e^{i2\phi} E'(t) \cos \theta, \quad (30)$$

with

$$E'(t) = H - \frac{H_e}{1+z} + \frac{1}{1+z} \int_0^z H(z') dz'. \quad (31)$$

The presence of $E(\eta)$ or $E'(t)$ is due to the variation of A_{jk} as well as the coupling of the background curvature with A_{jk} ; refer to Eq. (8). Now, it is ready to determine the modified GW waveform.

C. The Weyl tensor

In the previous subsection, the GW has been calculated, taking into account the corrections to the leading order short-wavelength approximation. However, \bar{h}_{jk} is not the variable which is directly measured by the interferometer. For the ground-based detectors, the strain $h = -2D^{jk} \int dt \int dt' R_{tjtk}^{\text{gw}}$ is measured, where D^{jk} is the detector configuration tensor [36]. In fact, it is the Weyl tensor component Ψ_4 that is gauge invariant, and gives the GW strain. Since the measurement takes place in the region where the cosmological evolution again plays little role, one can calculate Ψ_4 , assuming the flat spacetime background. So formally, Eqs. (11) - (14) still define a valid tetrad basis with η and r now representing the physical time and distance, respectively. In addition, γ_0 should be replaced by $2\pi f$. To calculate Ψ_4 , one defines a complex null vector field

$$\begin{aligned} m^\mu &= \frac{1}{\sqrt{2}} (x^\mu - iy^\mu) \\ &= \frac{1}{\sqrt{2}r} (0, 0, 1, -i \csc \theta). \end{aligned} \quad (32)$$

Note that in this expression, we do not put tildes above the symbols x and y , because in this case, the Minkowski metric is the physical one. m^μ and its complex conjugate \bar{m}^μ , together with l^μ and n^μ , form a Newman-Penrose (NP) tetrad basis [53, 54], which facilitates the calculation of Ψ_4 .

More specifically, Ψ_4 is one component of the Weyl tensor $C_{\mu\nu\rho\sigma}$, i.e. [54],

$$\Psi_4 = C_{\mu\nu\rho\sigma} n^\mu \bar{m}^\nu n^\rho \bar{m}^\sigma, \quad (33)$$

whose real part $\Re \Psi_4$ represents the $+$ polarization, and whose imaginary part $\Im \Psi_4$ corresponds to the \times polarization. At the leading order [$O(1/\epsilon^2)$], the Riemann tensor for the GW is given by [55]

$${}^{[1]}R_{\mu\nu\rho\sigma}^{\text{gw}} = -2\Re(l_{[\mu} A_{\nu]} l_{[\rho} J_{\sigma]} e^{-i\Phi}), \quad (34)$$

which is actually the leading order Weyl tensor ${}^{[1]}C_{abcd}^{\text{gw}}$. With this, one can easily calculate the leading order NP variable Ψ_4 , i.e.,

$$\Psi_4^{(1)} = \frac{1}{2}\Re(A^+ e^{-i\Phi}) + \frac{i}{2}\Re(A^\times e^{-i\Phi}), \quad (35)$$

where A^+ and A^\times are given by

$$A^+ = -\mathcal{A}e^{i2\phi} \frac{1 + \cos^2\theta}{2}, \quad A^\times = -i\mathcal{A}e^{i2\phi} \cos\theta, \quad (36)$$

respectively. So at this order, the Weyl tensor for the GW is given by [56]

$$C_{\mu\nu\rho\sigma}^{\text{gw}} = 2\Re(\Psi_4^{(1)} l_\mu \wedge m_\nu \wedge l_\rho \wedge m_\sigma), \quad (37)$$

with \wedge the wedge product. Let the detector carry its own coordinate system $\{t, X^{\hat{j}}\}$ with the two arms of the interferometer pointing in the \hat{X} and \hat{Y} directions, which are two arbitrary unit vectors, perpendicular to each other. Then, the electric part of the Weyl tensor is

$$\begin{aligned} C_{0\hat{j}0\hat{k}}^{\text{gw}} &= C_{\mu\nu\rho\sigma}^{\text{gw}} (\partial_t)^\mu (\partial_{\hat{j}})^\nu (\partial_t)^\rho (\partial_{\hat{k}})^\sigma \\ &= 2(2\omega)^2 \Re(\Psi_4^{(1)} m_{\hat{j}} m_{\hat{k}}) \\ &= (2\omega)^2 (\Re\Psi_4^{(1)} e_{\hat{j}\hat{k}}^+ + \Im\Psi_4^{(1)} e_{\hat{j}\hat{k}}^\times), \end{aligned} \quad (38)$$

where $(\partial_0)^\mu = (\partial/\partial t)^\mu$, $(\partial_{\hat{j}})^\mu = (\partial/\partial X^{\hat{j}})^\mu$, and $m_{\hat{j}} = m_\mu (\partial_{\hat{j}})^\mu$. $e_{\hat{j}\hat{k}}^P$ are the polarization matrices in the detector frame. The strain is thus given by [36]

$$\begin{aligned} h(t) &= -2D^{\hat{j}\hat{k}} \int dt' \int dt'' C_{0\hat{j}0\hat{k}}^{\text{gw}} \\ &= 2(\Re\Psi_4 F^+ + \Im\Psi_4 F^\times), \end{aligned} \quad (39)$$

where $D^{\hat{j}\hat{k}} = (\hat{X}^{\hat{j}} \hat{X}^{\hat{k}} - \hat{Y}^{\hat{j}} \hat{Y}^{\hat{k}})/2$ is the detector configuration matrix, and F^+ and F^\times are the antenna pattern functions for the + and the \times polarizations, respectively [57],

$$F^P = D^{\hat{j}\hat{k}} e_{\hat{j}\hat{k}}^P. \quad (40)$$

One recognizes $h^+ = A^+ e^{-i\Phi}$ and $h^\times = A^\times e^{-i\Phi}$ very easily from Eq. (35).

At the next leading order [$O(1/\epsilon)$], the Weyl tensor is given by a somewhat more complicated expression [58–62],

$$\begin{aligned} \Psi_4^{(2)} &= \frac{1}{2}\Re(B^+ e^{-i\Phi}) + \frac{i}{2}\Re(B^\times e^{-i\Phi}) \\ &\quad + \frac{2\bar{\mu} + 5\gamma - 3\bar{\gamma}}{2} [\Im(A^+ e^{-i\Phi}) + i\Im(A^\times e^{-i\Phi})] \\ &\quad + n^a [\Im(e^{-i\Phi} \nabla_a A^+) + i\Im(e^{-i\Phi} \nabla_a A^\times)], \end{aligned} \quad (41)$$

where $\sigma = -m^\mu m^\nu \nabla_\nu l_\mu$, $\gamma = (l^\mu n^\nu \nabla_\nu n_\mu - m^\mu n^\nu \nabla_\nu \bar{m}_\mu)/2$, and $\mu = \bar{m}^\mu m^\nu \nabla_\nu n_\mu$ are the spin coefficients of the flat metric in the spherical coordinate system

[54], \Im stands for the imaginary part, and the overhead bar indicates the complex conjugation. The straightforward calculation shows that these spin coefficients decay as $1/r^5$, so the second line in Eq. (41) can be ignored, as it does not represent the radiation. Then one obtains

$$\begin{aligned} \Psi_4^{(2)} &= \frac{1}{2}\Re \left[-i \left(\frac{E'}{4\pi f} + \Upsilon \right) A^+ e^{-i\Phi} \right] \\ &\quad + \frac{i}{2}\Re \left[-i \left(\frac{E'}{4\pi f} + \Upsilon \right) A^\times e^{-i\Phi} \right]. \end{aligned} \quad (42)$$

Here, the symbol Υ is

$$\Upsilon = \frac{32}{5} (\pi \mathcal{M} f)^{5/3} - \frac{H}{4\pi f}, \quad (43)$$

which comes from the third line in Eq. (41).

Finally, Ψ_4 is given by

$$\begin{aligned} \Psi_4 &= \Psi_4^{(1)} + \Psi_4^{(2)} \\ &= \frac{1}{2}\Re \left\{ \left[1 - i \left(\frac{E'}{4\pi f} + \Upsilon \right) \right] A^+ e^{-i\Phi} \right\} \\ &\quad + \frac{i}{2}\Re \left\{ \left[1 - i \left(\frac{E'}{4\pi f} + \Upsilon \right) \right] A^\times e^{-i\Phi} \right\}, \end{aligned} \quad (44)$$

up to the order $O(\epsilon)$. By comparing this expression with Eq. (35), one can redefine the amplitudes A^P and the phase Φ such that Eq. (44) takes the same form as Eq. (35). Therefore, the modified amplitudes and phase are

$$A'^P = \sqrt{1 + \left(\frac{E'}{4\pi f} + \Upsilon \right)^2} A^P, \quad (45)$$

$$\Phi' = \Phi + \arctan \left(\frac{E'}{4\pi f} + \Upsilon \right). \quad (46)$$

Since both $E'/4\pi f$ and Υ are small quantities, one may ignore the correction to the amplitudes. However, because of the sensitivity of the interferometers to the phase, one wants to keep the correction to the phase and approximates it as

$$\begin{aligned} \Phi' &\approx \Phi + \frac{E'}{4\pi f} + \Upsilon \\ &= \Phi - \frac{1}{4\pi f} \left[H + \frac{H_e}{1+z} - \frac{1}{1+z} \int_0^z H(z') dz' \right] \\ &\quad + \frac{32}{5} (\pi \mathcal{M} f)^{5/3}. \end{aligned} \quad (47)$$

Therefore, the correction to the phase consists of two parts, formally. One is given by the terms in the square brackets, which decreases with the frequency f and conforms to the short-wavelength approximation. The second part is the last term. This one actually is a monotonically increasing function of the frequency f , due to the increase in the power of the GW radiation. In fact, there is yet a hidden correction to the phasing, which

is the modified time dependence of the frequency f as nicely derived in Ref. [45]. This hidden correction will be briefly reviewed in the next section, and then, one finds out that it explicitly shows up in the Fourier transform of the phase.

III. THE FOURIER TRANSFORM

In this section, the Fourier transform of the GW will be found, which is used for the matched filtering [63]. First, we will review how the measured GW frequency varies with the time, based on the discussion in Ref. [45]. In this review, we ignore the peculiar motion of the binary system and the inhomogeneities of the universe. Second, we will derive the Fourier transform of the waveform represented by Eqs. (45) and (47).

A. The time dependence of the frequency

When taking the Fourier transformation of the time domain waveform, it is very important to know how the GW frequency f varies with time t . In the local Lorentz frame of the binary system, the GW frequency f_e follows

$$\frac{df_e}{dt_e} = \frac{96}{5} \frac{f_e}{\mathcal{M}_e} (\pi \mathcal{M}_e f_e)^{8/3}, \quad (48)$$

at the leading post-Newtonian order. From this, one can calculate the phase Φ in terms of $f = f_e/(1+z)$,

$$\Phi = -\frac{(\pi \mathcal{M} f)^{-5/3}}{16} + \Phi_c. \quad (49)$$

Since $dt = (1+z)dt_e$, one gets the equation satisfied by f ,

$$\frac{d}{dt} [(1+z)f] = \frac{96}{5} \frac{(1+z)f}{\mathcal{M}} (\pi \mathcal{M} f)^{8/3}, \quad (50)$$

$$\begin{aligned} f' &= \frac{d\Phi'}{dt} \\ &= f + \frac{3}{8f} \left[\frac{256}{5\mathcal{M}} (\pi \mathcal{M} f)^{8/3} - 2X \right] \left[\frac{5H}{4\pi} - \frac{H_e}{1+z} + \frac{1}{1+z} \int_0^z H(z') dz' \right] - \frac{3968}{5} (1+z) (\pi \mathcal{M} f)^{5/3} X \\ &\quad - \frac{1}{f} \left[\frac{5}{4\pi} \frac{dH}{dt} - \frac{1}{(1+z)^2} \frac{dH_e}{dt_e} + 2X \left(H + \frac{H_e}{1+z} \right) - \frac{2X}{1+z} \int_0^z H(z') dz' \right] + \frac{2048}{5\mathcal{M}} (1+z) (\pi \mathcal{M} f)^{13/3}. \end{aligned} \quad (56)$$

To obtain this expressions, one uses the following useful

from Eq. (48). In the usual approach, one sets z to be a constant, so one can take it out of the time derivative on the left hand side of the above expression, such that f evolves with t exactly the same way as f_e does with t_e , with appropriate rescaling of some quantities by powers of $(1+z)$. This is a good approximation because of the much faster orbital evolution than the cosmological expansion. However, if one wants to calculate the corrections to this approximation, the result is different. Directly integrating Eq. (50) leads to

$$[(1+z)f]^{-8/3} = \frac{256}{5} \frac{(\pi \mathcal{M}_e)^{8/3}}{\mathcal{M}_e} \int_t^{t_e} \frac{a(t'_e)}{a(t')} dt'. \quad (51)$$

During the lifetime of the binary system, the scale factor a changes by a small amount, so one can approximate it in the following way,

$$a(t'_e) \approx a(t_e) + (t'_e - t_e) \frac{da(t_e)}{dt_e}, \quad (52)$$

$$a(t') \approx a(t) + (t' - t) \frac{da(t)}{dt}. \quad (53)$$

Substituting these into Eq. (51) and ignoring higher order terms in $(t' - t)$ and $(t'_e - t_e)$, one obtains

$$f = \frac{1}{\pi \mathcal{M}} \left(\frac{256\tau}{5\mathcal{M}} \right)^{-3/8} \left[1 + \frac{3}{8} X(z)\tau \right], \quad (54)$$

where $\tau = t_c - t$, and

$$X(z) = \frac{1}{2} \left(H - \frac{H_e}{1+z} \right). \quad (55)$$

The second term in the square brackets in Eq. (54) represents the effect of the cosmological evolution on the time dependence of f .

In the above discussion, one does not consider the dephasing given in Eq. (47). Once this dephasing is taken into account, the effective GW frequency is

results,

$$\frac{dz}{dt} = 2(1+z)X, \quad (57)$$

$$\frac{dX}{dt} = \frac{1}{2} \left[\frac{dH}{dt} - \frac{1}{(1+z)^2} \frac{dH_e}{dt_e} + \frac{2H_e X}{1+z} \right], \quad (58)$$

$$\frac{df}{dt} = \frac{3f}{4} \left[\frac{128}{5\mathcal{M}} (\pi \mathcal{M} f)^{8/3} - X \right], \quad (59)$$

which can be easily obtained via straight forward but tedious calculations. Therefore, inspecting Eq. (56) shows that the corrections to the effective GW frequency f' are of the higher order, and one simply approximates $f' \approx f$ in the following.

B. The stationary-phase approximation

The Fourier transformation of the time-domain GW can be done using the stationary-phase approximation, i.e., the saddle point approximation [63, 64]. This is due to the much faster changing phase Φ' relative to the amplitudes A'^P .

Let us start with the Fourier transformation of a generic signal $s(t) = \Re\{\hat{A}(t)e^{-i\hat{\Phi}(t)}\}$, whose phase $\hat{\Phi}(t)$ varies with time t rapidly. The Fourier transformation is

$$\tilde{s}(F) = \int_{-\infty}^{\infty} \hat{A}(t)e^{i(2\pi Ft - \hat{\Phi}(t))} dt. \quad (60)$$

The saddle point t_s is determined by the extreme of the exponent in the integrand, $2\pi F - d\hat{\Phi}(t_s)/dt = 0$, i.e., $f_s \equiv d\hat{\Phi}(t_s)/dt = F$. One can then carry out the above integration in the frequency domain, i.e., replacing $dt = df/f$. Also, one expands the exponent around the saddle point f_s , so

$$\tilde{s}(f_s) = \int_{-\infty}^{\infty} \frac{\hat{A}(t)}{f} \times \exp\left\{i\left[2\pi f_s t_s - \hat{\Phi}_s - \frac{f_s^2}{2}(f - f_s)^2\right]\right\} df, \quad (61)$$

where $\hat{\Phi}_s \equiv \hat{\Phi}(t_s)$, and t in the above expression are taken to be an implicit function of f . Simply carrying out the integration gives

$$\tilde{s}(F) = \frac{\hat{A}(t_s)}{\sqrt{f_s}} \exp\left[i\left(2\pi f_s t_s - \hat{\Phi}_s - \frac{\pi}{4}\right)\right], \quad (62)$$

from which, one can read off the phase of the Fourier transformed signal,

$$\tilde{\Phi} = 2\pi f_s t_s - \hat{\Phi}_s - \frac{\pi}{4}, \quad (63)$$

with t_s an implicit function of f_s . So if one knows the dependence of the frequency f_s on t_s , one can invert it to obtain $t_s = t_s(f_s)$.

Applying this general prescription to the GW strain (45) and (47), one finds out that the Fourier transformed GW has the following phase,

$$\begin{aligned} \tilde{\Phi}' = & 2\pi f t_c - \Phi_c - \frac{\pi}{4} + \frac{3}{128}(\pi \mathcal{M} f)^{-5/3} \\ & - \frac{25\mathcal{M}}{32 \cdot 768}(\pi \mathcal{M} f)^{-13/3} X(z) \\ & - \frac{1}{4\pi f} \left[H + \frac{H_e}{1+z} - \frac{1}{1+z} \int_0^z H(z') dz' \right] \\ & + \frac{32}{5}(\pi \mathcal{M} f)^{5/3}. \end{aligned} \quad (64)$$

The first line is the usual leading order phase presented in Ref. [65]. The second line was already given in Ref. [45], which is due to the modified time dependence of the measured GW frequency f , as result of the cosmological evolution of z . This term is formally at the -4 PN order. The last two lines are the corrections to the leading order short-wavelength approximation, where the third one is due to the cosmological evolution and formally, is at the 1PN order, and the fourth line comes from the orbital decay of the binary system and is at the 5PN order. By setting f to be the GW frequency corresponding to the inner most stable orbit [45]

$$f_{\text{isco}} = 8.80(1 + 1.25\eta + 1.08\eta^2) \left[\frac{M_{\odot}}{(1+z)(m_1 + m_2)} \right] \text{kHz}, \quad (65)$$

with $\eta = m_1 m_2 / (m_1 + m_2)^2$, the 5PN order correction contributes

$$\Delta\Phi_{5\text{PN}}^{\text{max}} \approx 0.099 \quad (66)$$

at most up to the frequency f_{isco} . Figure 1 shows the dephasing $\Delta\Phi$, to be accumulated from some initial observation frequency f to f_{isco} , due to the 5PN correction for different types of sources defined in Table I. These sources include the binary star systems observed in GW150914 and GW170817 for the ground-based interferometers [7], and the sources for the space-borne detectors: the extreme mass-ratio inspiral (EMRI), the intermediate mass-ratio inspiral (IMRI), the intermediate mass black hole binary (IMBH) and the supermassive black hole binary (SMBH) [66]. From Fig. 1, one finds out that the $\Delta\Phi$ changes very slowly at the beginning, and rapidly decreases when f_{isco} is approached. In addition, this phase correction $\Delta\Phi$ is very sensitive to the symmetric mass ratio η . Binary systems with very similar components have much greater dephasing $\Delta\Phi$ than those with distinct components.

As discussed in Ref. [45], the -4 PN correction to the GW phase is very difficult to be detected by the ground-based interferometers, such as LIGO/Virgo. This term is slightly larger for GWs in the LISA band, but even with a template not considering this effect, the mismatch is less than 10^{-3} . This is due to the extreme smallness of $X(z)$ [refer to Eq. (55)]. Similarly, the correction at 1PN is also highly suppressed by the small Hubble parameters, so it would be even more difficult to be detected. Finally, the 5PN correction also induces a small mismatch, which will be calculated in the next subsection.

C. Mismatch

In this subsection, the mismatch due to the 5PN correction is calculated [67]. Although currently, the complete waveform at the 5PN has not yet been analytically calculated from the first principle, several phenomenological models exist, which contain terms at and beyond the 5PN order, such as IMRPhenomD [68, 69]. In

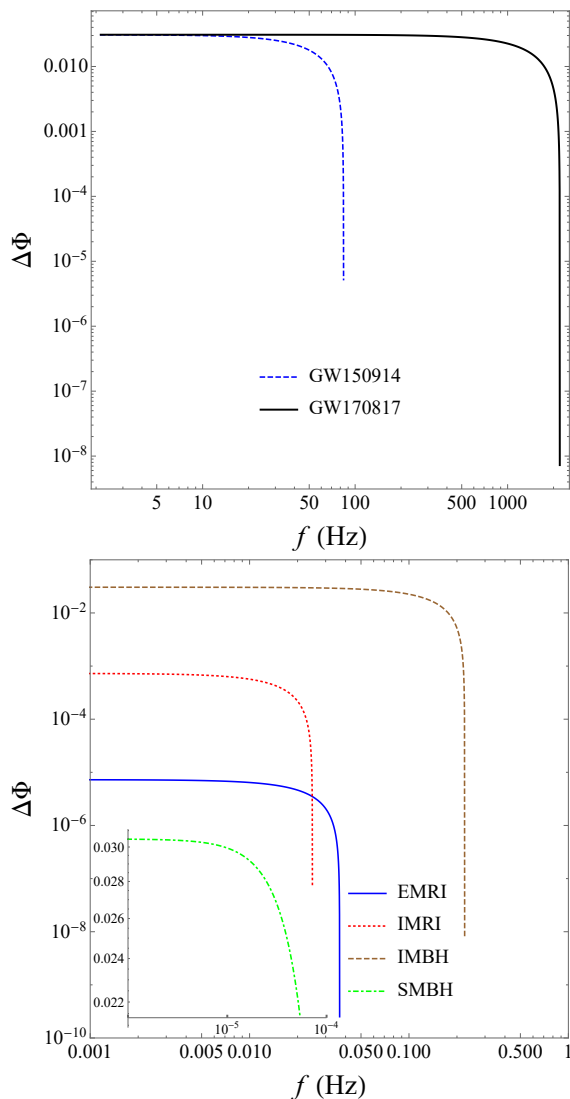


FIG. 1. The dephasing $\Delta\Phi$ to be accumulated due to the 5PN correction as a function of the initial observation frequency f . The upper panel shows $\Delta\Phi$ for GW150914 and GW170817 [7]. The lower panel shows $\Delta\Phi$ for sources defined in Table I.

this model, the terms of the order higher than 3.5PN in the phase for the inspiral stage were introduced in Eq. (28) as the ansatz. Those higher order terms carry certain phenomenological coefficients, which were fixed by fitting it to the hybrid effective-one-body–numerical-relativity waveforms. The numerical values for those phenomenological coefficients are further related to the physical quantities, such as the symmetric mass ratio η and a spin parameter χ_{PN} [defined in Eq. (3)], by Eq. (31) in Ref. [69], where a new set of coefficients λ_{ij} are introduced and tabulated in Table V. One can find out that the coefficients λ_{ij} for the 5PN term (in the row with σ_3) have very large absolute values compared to that of the 5PN order correction found in the current work. So the mismatch caused by the 5PN correction should be small.

In order to calculate the mismatch, the fitting factor

FF between two waveforms h_1 and h_2 are needed. Suppose these waveforms are described by a certain number of parameters θ^a , then FF is defined to be

$$FF = \max_{\Delta\theta^a} \frac{\langle h_1 | h_2 \rangle}{\|h_1\| \|h_2\|}, \quad (67)$$

where $\Delta\theta^a$ represent the differences between the parameters of the waveforms, and the numerator on the right hand side is an inner product

$$\langle h_1 | h_2 \rangle = 4\Re \int_0^\infty \frac{\tilde{h}_1^*(f) \tilde{h}_2(f)}{S_n(f)} df, \quad (68)$$

with \tilde{h}_1 and \tilde{h}_2 the Fourier transformed waveforms, and $S_n(f)$ the one-sided noise power spectrum of the interferometer. With this inner product, one defines $\|h_1\| = \sqrt{\langle h_1 | h_1 \rangle}$ and $\|h_2\| = \sqrt{\langle h_2 | h_2 \rangle}$. The mismatch is thus given by [67]

$$\mathfrak{M} = 1 - FF, \quad (69)$$

which quantifies the difference between h_1 and h_2 .

In our calculation, we take \tilde{h}_1 to be a simplified IMR-PhenomD waveform whose amplitude is given by

$$A \propto \eta^{1/2} (Mf)^{-7/6}, \quad (70)$$

which is actually the leading order GW amplitude calculated by considering the quadruple radiation only. The exact proportionality factor is not important for calculating the mismatch. The phase of \tilde{h}_1 is given by

$$\begin{aligned} \phi_{\text{Ins}} = & 2\pi f t_c - \Phi_c - \frac{\pi}{4} \\ & + \frac{3}{128} (\pi M f)^{-5/3} \sum_{j=0}^7 \varphi_j (\pi M f)^{j/3} \\ & + \frac{1}{\eta} \left[\sigma_0 + \sigma_1 M f + \frac{3}{4} \sigma_2 (M f)^{4/3} + \frac{3}{5} \sigma_3 (M f)^{5/3} \right], \end{aligned} \quad (71)$$

where the second line includes the fourth term in Eq. (64) and higher PN order corrections up to 3.5PN, and the third line includes even higher PN order terms up to 5PN. The third line is actually the phase ansatz introduced in Ref. [69]. The expressions for the factors φ_j and σ_k are given in Ref. [69]. Although these factors also depend on the spins, we ignore them, i.e., set all spins to zero. So the parameters describing the waveform \tilde{h}_1 are M, η, t_c and Φ_c . We also ignore the phases for the intermediate and the merger-ringdown stages as discussed in Ref. [69]. Finally, the waveform \tilde{h}_2 is basically \tilde{h}_1 modified by the 5PN phase correction given by the last term in Eq. (64).

We consider the mismatch between the two waveforms observed by the ground-based detectors [aLIGO, Virgo, KAGRA, Einstein Telescope (ET) [26] and Cosmic Explorer (CE) [70]] and the space-borne detector (LISA [71]). In carrying out the integrations, we set the lower

integration limit f_{\min} for the ground-based detectors to be 1 Hz if Einstein Telescope is used and 5 Hz if other detectors are used. The upper integration limit is given by $f_{\max} = 0.018/M$ according to the construction of the inspiral phase in Ref. [69]. For LISA, the lower integration limit is chosen to be $f_{\min} = 10^{-4}$ Hz, and the upper

limit is

$$f_{\max} = \min(f_{\text{isco}}, f_{4\text{yr}}). \quad (72)$$

Here, $f_{4\text{yr}}$ is the GW frequency evolving from f_{\min} in 4 years, approximately given by,

$$f_{4\text{yr}} = \left[f_{\min}^{-8/3} - \frac{256\pi}{5} (\pi\mathcal{M})^{5/3} \Delta t \right]^{-3/8}, \quad (73)$$

with $\Delta t = 4$ years.

	$m_1(M_\odot)$	$m_2(M_\odot)$	z	d_L (Mpc)	Mismatches					
					aLIGO	Virgo	KAGRA	ET	CE	LISA
GW150914	35.6	30.6	0.09	424	2.48×10^{-6}	2.29×10^{-6}	2.02×10^{-6}	3.76×10^{-6}	5.90×10^{-6}	-
GW170817	1.46	1.27	0.01	45	9.61×10^{-7}	8.54×10^{-7}	5.76×10^{-7}	4.06×10^{-6}	9.95×10^{-9}	-
EMRI	10^5	10	0.20	1000	-	-	-	-	-	6.05×10^{-13}
IMRI	10^5	10^3	0.78	5000	-	-	-	-	-	1.42×10^{-8}
IMBH	5×10^3	4×10^3	2.0	1.6×10^4	-	-	-	-	-	3.55×10^{-15}
SMBH	5×10^6	4×10^6	5.0	4.8×10^4	-	-	-	-	-	7.86×10^{-8}

TABLE I. Parameters for different types of GW sources (columns 2 - 5), and the mismatches for different detectors (columns 6 - 11). The parameter values for GW150914 and GW170817 are taken from Ref. [7], and these in the last four rows are suggested by Ref. [66].

In the calculation, we let the parameters for \tilde{h}_1 be given by the equivalent ones listed in the columns 2 to 5 in Table I. The values for t_c and Φ_c play no role in the mismatch, so neither of them is listed. The parameters for \tilde{h}_2 differ from those for \tilde{h}_1 by $\Delta\theta^a = (\Delta\mathcal{M}, \Delta\eta, \Delta t_c, \Delta\Phi_c)$. Note that, Δt_c and $\Delta\Phi_c$ need to be specified in the calculation. Using the MATLAB function `fmincon` for finding the minimum of a constrained function (since $0 < \eta \leq 0.25$), one can calculate all the mismatches for different detectors. These values are also tabulated from column 6 to 11 in Table I. One finds out that the mismatches are very small, less than $10^{-5} \sim 10^{-6}$. Although our 5PN order correction may seem to be negligible, it should be considered in the more accurate measurements of GWs.

IV. CONCLUSION

In this work, we considered the corrections to the leading order short-wavelength approximation, by taking into account the temporal and the spatial variation of the GW amplitude. The variation is mainly due to the orbital

decay of the binary star system; the cosmological evolution also modifies the amplitude, but its impact is much smaller. The evolution equations for the leading and the subleading order amplitudes were obtained, and these amplitudes were then computed for the GW generated by a binary system. The Weyl tensor component Ψ_4 was calculated to reveal the modifications to the waveform, in particular, the dephasing. After the Fourier transformation, the dephasing consists of three contributions. The first is at the -4PN , which was analyzed in Refs. [43–45]. The second is at the 1PN . Both of these carry factors containing the source redshift z and the Hubble parameters, but they are too small to be easily detected. The final contribution to the dephasing is at the 5PN order, which should be taken into account for the more accurate computation of the GW.

ACKNOWLEDGMENTS

This work was supported by the National Natural Science Foundation of China under Grants Nos. 11633001 and the Strategic Priority Research Program of the Chinese Academy of Sciences, Grant No. XDB23000000.

- [1] B. P. Abbott *et al.* (Virgo, LIGO Scientific), *Phys. Rev. Lett.* **116**, 061102 (2016), [arXiv:1602.03837 \[gr-qc\]](#).
- [2] B. P. Abbott *et al.* (Virgo, LIGO Scientific), *Phys. Rev. Lett.* **116**, 241103 (2016), [arXiv:1606.04855 \[gr-qc\]](#).
- [3] B. P. Abbott *et al.* (Virgo, LIGO Scientific), *Phys. Rev. Lett.* **118**, 221101 (2017), [arXiv:1706.01812 \[gr-qc\]](#).
- [4] B. P. Abbott *et al.* (Virgo, LIGO Scientific), *Phys. Rev. Lett.* **119**, 141101 (2017), [arXiv:1709.09660 \[gr-qc\]](#).
- [5] B. P. Abbott *et al.* (Virgo, LIGO Scientific), *Phys. Rev. Lett.* **119**, 161101 (2017), [arXiv:1710.05832 \[gr-qc\]](#).
- [6] B. P. Abbott *et al.* (Virgo, LIGO Scientific), *Astrophys. J.* **851**, L35 (2017), [arXiv:1711.05578 \[astro-ph.HE\]](#).
- [7] B. P. Abbott *et al.* (LIGO Scientific, Virgo), *Phys. Rev. X* **9**, 031040 (2019), [arXiv:1811.12907 \[astro-ph.HE\]](#).
- [8] A. Einstein, *Sitzungsber. Preuss. Akad. Wiss. Berlin (Math. Phys.)* **1916**, 688 (1916); **1918**, 154 (1918).
- [9] C. M. Will, *Living Rev. Rel.* **17**, 4 (2014), [arXiv:1403.7377 \[gr-qc\]](#).
- [10] S. Hou, Y. Gong, and Y. Liu, *Eur. Phys. J. C* **78**, 378 (2018), [arXiv:1704.01899 \[gr-qc\]](#).
- [11] Y. Gong, S. Hou, D. Liang, and E. Papantonopoulos, *Phys. Rev. D* **97**, 084040 (2018), [arXiv:1801.03382 \[gr-qc\]](#).
- [12] Y. Gong and S. Hou, *Universe* **4**, 85 (2018), [arXiv:1806.04027 \[gr-qc\]](#).
- [13] K. Somiya (KAGRA), *Gravitational waves. Numerical relativity - data analysis. Proceedings, 9th Edoardo Amaldi Conference, Amaldi 9, and meeting, NRDA 2011, Cardiff, UK, July 10-15, 2011, Class. Quant. Grav.* **29**, 124007 (2012), [arXiv:1111.7185 \[gr-qc\]](#).
- [14] Y. Aso, Y. Michimura, K. Somiya, M. Ando, O. Miyakawa, T. Sekiguchi, D. Tatsumi, and H. Yamamoto (KAGRA), *Phys. Rev. D* **88**, 043007 (2013), [arXiv:1306.6747 \[gr-qc\]](#).
- [15] A. Goldstein *et al.*, *Astrophys. J.* **848**, L14 (2017), [arXiv:1710.05446 \[astro-ph.HE\]](#).
- [16] V. Savchenko *et al.*, *Astrophys. J.* **848**, L15 (2017), [arXiv:1710.05449 \[astro-ph.HE\]](#).
- [17] B. P. Abbott *et al.* (Virgo, Fermi-GBM, INTEGRAL, LIGO Scientific), *Astrophys. J.* **848**, L13 (2017), [arXiv:1710.05834 \[astro-ph.HE\]](#).
- [18] T. Baker, E. Bellini, P. G. Ferreira, M. Lagos, J. Noller, and I. Sawicki, *Phys. Rev. Lett.* **119**, 251301 (2017), [arXiv:1710.06394 \[astro-ph.CO\]](#).
- [19] P. Creminelli and F. Vernizzi, *Phys. Rev. Lett.* **119**, 251302 (2017), [arXiv:1710.05877 \[astro-ph.CO\]](#).
- [20] J. Sakstein and B. Jain, *Phys. Rev. Lett.* **119**, 251303 (2017), [arXiv:1710.05893 \[astro-ph.CO\]](#).
- [21] J. M. Ezquiaga and M. Zumalacárregui, *Phys. Rev. Lett.* **119**, 251304 (2017), [arXiv:1710.05901 \[astro-ph.CO\]](#).
- [22] A. Emir Gümrukçüoğlu, M. Saravani, and T. P. Sotiriou, *Phys. Rev. D* **97**, 024032 (2018), [arXiv:1711.08845 \[gr-qc\]](#).
- [23] J. Oost, S. Mukohyama, and A. Wang, *Phys. Rev. D* **97**, 124023 (2018), [arXiv:1802.04303 \[gr-qc\]](#).
- [24] Y. Gong, S. Hou, E. Papantonopoulos, and D. Tzortzis, *Phys. Rev. D* **98**, 104017 (2018), [arXiv:1808.00632 \[gr-qc\]](#).
- [25] X. Gao and X.-Y. Hong, (2019), [arXiv:1906.07131 \[gr-qc\]](#).
- [26] M. Punturo *et al.*, *Gravitational waves. Proceedings, 8th Edoardo Amaldi Conference, Amaldi 8, New York, USA, June 22-26, 2009, Class. Quant. Grav.* **27**, 084007 (2010).
- [27] C. Caprini and D. G. Figueroa, *Class. Quant. Grav.* **35**, 163001 (2018), [arXiv:1801.04268 \[astro-ph.CO\]](#).
- [28] M. Maggiore, *Gravitational Waves. Vol. 1: Theory and Experiments*, Oxford Master Series in Physics (Oxford University Press, 2007).
- [29] R. A. Isaacson, *Phys. Rev.* **166**, 1263 (1968).
- [30] J. K. Lawrence, *Il Nuovo Cimento B* (1971-1996) **6**, 225 (1971).
- [31] J. K. Lawrence, *Phys. Rev. D* **3**, 3239 (1971).
- [32] H. C. Ohanian, *Int. J. Theor. Phys.* **9**, 425 (1974).
- [33] R. Takahashi and T. Nakamura, *Astrophys. J.* **595**, 1039 (2003), [arXiv:astro-ph/0305055 \[astro-ph\]](#).
- [34] K. Liao, M. Biesiada, and X.-L. Fan, *Astrophys. J.* **875**, 139 (2019), [arXiv:1903.06612 \[gr-qc\]](#).
- [35] P. Schneider, J. Ehlers, and E. E. Falco, *Gravitational Lenses* (Springer, Berlin, Heidelberg, 1992) p. 560.
- [36] S. Hou, X.-L. Fan, and Z.-H. Zhu, *Phys. Rev. D* **100**, 064028 (2019), [arXiv:1907.07486 \[gr-qc\]](#).
- [37] S. Hou, X.-L. Fan, K. Liao, and Z.-H. Zhu, (2019), [arXiv:1911.02798 \[gr-qc\]](#).
- [38] B. F. Schutz, *Nature* **323**, 310 (1986).
- [39] D. E. Holz and S. A. Hughes, *Astrophys. J.* **629**, 15 (2005), [arXiv:astro-ph/0504616 \[astro-ph\]](#).
- [40] B. P. Abbott *et al.* (LIGO Scientific, Virgo, 1M2H, Dark Energy Camera GW-E, DES, DLT40, Las Cumbres Observatory, VINROUGE, MASTER), *Nature* **551**, 85 (2017), [arXiv:1710.05835 \[astro-ph.CO\]](#).
- [41] B. P. Abbott *et al.* (LIGO Scientific, Virgo), (2019), [arXiv:1908.06060 \[astro-ph.CO\]](#).
- [42] H.-Y. Chen, M. Fishbach, and D. E. Holz, *Nature* **562**, 545 (2018), [arXiv:1712.06531 \[astro-ph.CO\]](#).
- [43] N. Seto, S. Kawamura, and T. Nakamura, *Phys. Rev. Lett.* **87**, 221103 (2001), [arXiv:astro-ph/0108011 \[astro-ph\]](#).
- [44] A. Nishizawa, K. Yagi, A. Taruya, and T. Tanaka, *Phys. Rev. D* **85**, 044047 (2012), [arXiv:1110.2865 \[astro-ph.CO\]](#).
- [45] C. Bonvin, C. Caprini, R. Sturani, and N. Tamanini, *Phys. Rev. D* **95**, 044029 (2017), [arXiv:1609.08093 \[astro-ph.CO\]](#).
- [46] C. Messenger and J. Read, *Phys. Rev. Lett.* **108**, 091101 (2012), [arXiv:1107.5725 \[gr-qc\]](#).
- [47] C. Messenger, K. Takami, S. Gossan, L. Rezzolla, and B. S. Sathyaprakash, *Phys. Rev. X* **4**, 041004 (2014), [arXiv:1312.1862 \[gr-qc\]](#).
- [48] K. Kawaguchi, K. Kiuchi, K. Kyutoku, Y. Sekiguchi, M. Shibata, and K. Taniguchi, *Phys. Rev. D* **97**, 044044 (2018), [arXiv:1802.06518 \[gr-qc\]](#).
- [49] S. Weinberg, *Cosmology* (Oxford, UK: Oxford Univ. Pr. (2008) 593 p, 2008).
- [50] V. Mukhanov, *Physical Foundations of Cosmology* (Cambridge University Press, Oxford, 2005).
- [51] C. W. Misner, K. S. Thorne, and J. A. Wheeler, *Gravitation* (W. H. Freeman, San Francisco, 1973).
- [52] Note that this l^0 is the time component of the *physical* wave vector.
- [53] E. Newman and R. Penrose, *J. Math. Phys.* **3**, 566 (1962), [Errata: *J. Math. Phys.* **4**, no. 7, 998 (1963)].

- [54] H. Stephani, D. Kramer, M. A. H. MacCallum, C. Hoenselaers, and E. Herlt, *Exact solutions of Einstein's field equations*, Cambridge Monographs on Mathematical Physics (Cambridge Univ. Press, Cambridge, 2003).
- [55] A. I. Harte, *Gen. Rel. Grav.* **51**, 14 (2019), [arXiv:1808.06203](https://arxiv.org/abs/1808.06203) [gr-qc].
- [56] S. Chandrasekhar, *The mathematical theory of black holes*, Oxford classic texts in the physical sciences (Oxford University Press, Oxford, 1998).
- [57] E. Poisson and C. M. Will, *Gravity: Newtonian, Post-Newtonian, Relativistic* (Cambridge University Press, 2014).
- [58] J. M. Martín-García, R. Portugal, and L. R. U. Manssur, *Comput. Phys. Commun.* **177**, 640 (2007), [arXiv:0704.1756](https://arxiv.org/abs/0704.1756) [cs.SC].
- [59] J. M. Martín-García, D. Yllanes, and R. Portugal, *Comput. Phys. Commun.* **179**, 586 (2008), [arXiv:0802.1274](https://arxiv.org/abs/0802.1274) [cs.SC].
- [60] J. M. Martín-García, *Comput. Phys. Commun.* **179**, 597 (2008).
- [61] D. Brizuela, J. M. Martín-García, and G. A. Mena Marugán, *Gen. Rel. Grav.* **41**, 2415 (2009), [arXiv:0807.0824](https://arxiv.org/abs/0807.0824) [gr-qc].
- [62] J. M. Martín-García, “*xAct*: Efficient tensor computer algebra for the wolfram language,” <http://www.xact.es/>, [Online; accessed May 19, 2017].
- [63] S. Droz, D. J. Knapp, E. Poisson, and B. J. Owen, *Phys. Rev. D* **59**, 124016 (1999), [arXiv:gr-qc/9901076](https://arxiv.org/abs/gr-qc/9901076) [gr-qc].
- [64] N. Yunes, K. G. Arun, E. Berti, and C. M. Will, *Phys. Rev. D* **80**, 084001 (2009), [Erratum: *Phys. Rev. D* **89**, no.10, 109901 (2014)], [arXiv:0906.0313](https://arxiv.org/abs/0906.0313) [gr-qc].
- [65] A. Buonanno, B. Iyer, E. Ochsner, Y. Pan, and B. S. Sathyaprakash, *Phys. Rev. D* **80**, 084043 (2009), [arXiv:0907.0700](https://arxiv.org/abs/0907.0700) [gr-qc].
- [66] K. Chamberlain and N. Yunes, *Phys. Rev. D* **96**, 084039 (2017), [arXiv:1704.08268](https://arxiv.org/abs/1704.08268) [gr-qc].
- [67] T. A. Apostolatos, *Phys. Rev. D* **52**, 605 (1995).
- [68] S. Husa, S. Khan, M. Hannam, M. Pürrer, F. Ohme, X. Jiménez Forteza, and A. Bohé, *Phys. Rev. D* **93**, 044006 (2016), [arXiv:1508.07250](https://arxiv.org/abs/1508.07250) [gr-qc].
- [69] S. Khan, S. Husa, M. Hannam, F. Ohme, M. Pürrer, X. Jiménez Forteza, and A. Bohé, *Phys. Rev. D* **93**, 044007 (2016), [arXiv:1508.07253](https://arxiv.org/abs/1508.07253) [gr-qc].
- [70] B. P. Abbott *et al.* (LIGO Scientific), *Class. Quant. Grav.* **34**, 044001 (2017), [arXiv:1607.08697](https://arxiv.org/abs/1607.08697) [astro-ph.IM].
- [71] P. A. Seoane *et al.* (eLISA), (2013), [arXiv:1305.5720](https://arxiv.org/abs/1305.5720) [astro-ph.CO].